Arabian Journal of Chemistry (2019) **12**, 1722–1732

King Saud University

Arabian Journal of Chemistry

www.ksu.edu.sa
www.sciencedirect.com

ORIGINAL ARTICLE

Green biosynthesis of silver nanoparticles using *Torreya nucifera* and their antibacterial activity

Duraisamy Kalpana [a], Jung Hoon Han [a], Whoa Shig Park [b], Seok Myon Lee [b], Rizwan Wahab [c], Yang Soo Lee [a,*]

[a] *Department of Forest Science and Technology, Institute of Agricultural Science and Technology, Chonbuk National University, Jeonju, South Korea*
[b] *Jeolla Namdo, Forest Resources Research Institute, South Korea*
[c] *College of Science, Department of Zoology, King Saud University, Riyadh 11451, Saudi Arabia*

Received 28 June 2013; accepted 16 August 2014
Available online 1 September 2014

KEYWORDS

Torreya nucifera;
Silver nanoparticles;
XRD;
FT-IR;
Salmonella typhimurium

Abstract Silver nanoparticles were biosynthesized with the aid of a novel and eco-friendly biological material *Torreya nucifera*. Temperature and extract concentration were found to influence the size and shape of the biosynthesized silver nanoparticles. Morphological images of biosynthesized nanomaterials revealed that the particles are in spherical shape and size ranging between 10 and 125 nm. Crystalline nature of nanoparticles in face centered cubic (fcc) structure was ensured by diffraction pattern peaks corresponding to (1 1 1), (2 0 0), (2 2 0) and (3 1 1) planes. Characterization of the biosynthesized nanoparticles was performed by the X-ray diffraction and Fourier Transform Infrared spectroscopy analyses. FT-IR analysis indicates that nanoparticles are bound to proteins through amine groups of the aminoacid. Furthermore the biosynthesized nanoparticles were found to be highly effective against *Salmonella typhimurium* bacterium, which validates its potential applications as antibacterial agents in drinking water treatment and in food packagings.

1. Introduction

Booming demand of nanostructured materials grabbed intensive attention from pharmaceutical, chemical, green energy and natural product sectors in which the connotation of metal nanoparticles is highly imperative. The high surface area, unique electrical and optical properties, target delivery etc., effectively haul its intensive applications in the mentioned fields. Metal nanoparticles find its applications in various fields like optoelectronics, information storage (Mazur, 2004; Singhal et al., 2009; Mishra et al., 2010; Avasthi et al., 2007) and in biological fields such as drug delivery, gene delivery, photodynamics and imaging (Jong and Born, 2008). In addition to the unique catalytic activity, electrical conductivity, and chemical stability exhibited by the noble metals, metallic silver also possesses antibacterial effects (Chernousova and Epple, 2013; Hetrick and Schoenfisch, 2006; Pallavicini et al., 2014).

* Corresponding author. Tel.: +82 9740 2622.
E-mail address: ysoolee@chonbuk.ac.kr (Y.S. Lee).
Peer review under responsibility of King Saud University.

Production and hosting by Elsevier

http://dx.doi.org/10.1016/j.arabjc.2014.08.016

Among the noble studied metals, nanometric silver is of great choice due to their superior biological and eco-friendly properties, as silver is not toxic for the human cells at low concentrations (Amato et al., 2011). The chitosan conjugated with silver oxide was found to possess antibacterial activity against *Staphylococcus aureus* (Hu et al., 2006) and silver alloy coated urinary catheters were demonstrated to prevent the urinary tract infection (Saint et al., 1998). The silver nanoparticles are widely used as catalyst, antimicrobial materials, in staining glasses, ceramics, in electronics and in surface enhanced Raman spectroscopy (SERS) (Capek, 2004). Silver nanoparticles are also utilized in medical fields as wound dressings and in the urinary catheters (Kim and Kim, 2006). Studies by Jain and Pradeep suggested the potential use of silver nanoparticles coated polyurethane foams as antibacterial water filter (Jain and Pradeep, 2005).

The general method for the synthesis of silver nanoparticles involves chemical reduction method, which utilizes sodium borohydride, citrate, ascorbate and hydrazine as reducing agents (Sileikaite et al., 2006; Ratyakshi and Chauhan, 2009; Solomon et al., 2007; Cao et al., 2010 and Zielinska et al., 2009; Mishra et al., 2007). The toxic chemical species adsorbed on the surface of nanoparticles may produce adverse effects in medical applications, which limit the chemical synthesis of nanoparticles (Parashar et al., 2009). The coating of nanoparticles with biomolecules will favor the interactions of nanoparticles with the biosystems (Amato et al., 2011). It necessitates the urge of bio-mediated nanoparticle synthesis. The commonly employed green synthesis methods are polysaccharide, Tollens, irradiated and biological methods (Sharma et al., 2009). Silver nanoparticles were synthesized using bacteria, yeast, and fungi (Saifuddin et al., 2009; Reddy et al., 2010; Ali et al., 2011; Gajbhije et al., 2009; Ahmad et al., 2003; Kowshik et al., 2003). Recently, the synthesis of metal nano particles using plant extracts has gained intensive importance. The extracts of *Chenopodium album* (Dwivedi and Gopal, 2010), *Rosa rugosa* (Dubey et al., 2010), *Aloe vera* (Chandran et al., 2006), *Azadirachta indica* (Shankar et al., 2004), and *Cinnamomum camphora* (Huang et al., 2007) plants have been potentially utilized to synthesize the silver and gold nanoparticles. Utilizing the plants for the synthesis of nanoparticles prevents the release of large quantities of toxic chemicals in solid, liquid and gaseous form to the environment (Dubey et al., 2010) and also it eliminates adherence of toxic substances on synthesized nanoparticles thereby increasing its applications in biomedical science. The size, morphology, stability, physical and chemical properties of nanoparticles play an important role in their applications. Tools are required to control the size and shape of metal nanostructures for enhancing their specific application similar to metals engineered to the macroscopic devices (Wiley et al., 2007). The size and shape of nanoparticles can be controlled by maintaining a set of reaction parameters like pH, temperature, concentration of metal solution and concentration of reducing agents. Many studies as presented above (Dwivedi and Gopal, 2010; Dubey et al., 2010; Chandran et al., 2006; Shankar et al., 2004; Huang et al., 2007) have been explored in synthesizing and characterizing the nanoparticles synthesized using various plant extracts, but only few studies were carried out on the effect of various parameters affecting the shape and size of nanoparticles. The morphology (size and shape) of nanoparticles plays an important role in their applications and interaction of the silver nanoparticles on the gram negative bacteria was found to be size dependent (Morones et al., 2005). The antibacterial activity of the nano particles was found to be highly dependent upon shape of nanoparticles (Pal et al., 2007).

Torreya nucifera, coniferous tree belongs to the Taxaceae family native to South Korea's Jeju Island and Southern Japan. It has been used traditionally in Asian medicine as a remedy for stomachache, hemorrhoids and rheumatoid arthritis (Bae, 2000). Its leaves possess antioxidant activity, (Lee et al., 2006) antiviral activity (Ryu et al., 2010) and neuro-protective activity (Jang et al., 2001), the capability of synthesizing nanoparticles is yet to be explored. Hence it has been planned to synthesize the silver nanoparticles using the biobased aqueous extract of *T. nucifera* leaves and study the antibacterial activity using gram-negative *Salmonella typhimurium* bacteria, commonly found on contaminated food and water leading to diarrhea, fever and gastric enteritis. Commonly *Escherichia coli* and *S. aureus* are used for determining the antibacterial activity in previous studies, so we selected *S. typhimurium* which also causes water contamination in the current study (Ailes et al., 2013). The present study utilizes *T. nucifera*, a nontoxic bioresource for synthesizing silver nanoparticles rapidly in a controlled manner. It also focuses on effects of temperature and concentration of extract in the determination of size and shape of biosynthesized nanoparticles.

2. Materials and methods

2.1. Materials

Silver nitrate (99%) was purchased from Sigma Aldrich and leaves of *T. nucifera* were collected from Wando Arboretum, Wando, South Korea.

2.2. Preparation of extract

Fresh and healthy *T. nucifera* leaves were collected, washed thoroughly with distilled water and dried for ten days. Then the leaves were cut into small pieces and powdered in a mixer. Two gram of powder was added to a 1000 ml round bottomed flask with 100 ml sterile distilled water and boiled for 15 min at 60 °C. Then the extract was filtered and collected filtrate was stored in refrigerator until the synthesis of silver nanoparticles was carried out.

2.3. Synthesis of silver nanoparticles

Ten milliliter of the aqueous extract was gradually added into 90 ml of aqueous solution of 1 mM silver nitrate ($AgNO_3$) in a 250 ml Erlenmeyer flask and incubated in a shaking incubator at 20 °C under dark conditions. The reaction mixture was checked at regular time intervals for monitoring the change in color of $AgNO_3$ solution from colorless to brown. The fully reduced solution was centrifuged at 15,000*g* for 30 min. The supernatant liquid was discarded and pellet obtained was redispersed in deionized water. The centrifugation process was repeated two to three times to wash off any adsorbed substances on the surface of silver nanoparticles.

2.4. Optimization of different parameters

2.4.1. Temperature

The above mentioned procedure was repeated for optimization of temperature, where the reaction temperature was maintained at 35, 50 and 65 °C for 9:1 ratios of silver nitrate and leaf extract solution. The absorbance of resulting solutions was measured spectro-photometrically.

2.4.2. Concentration ratio of leaf extract

The above mentioned procedure was also repeated to examine the impact of leaf extract concentration on the size and shape of silver nanoparticles. For the optimization, the reaction was monitored by using different ratios of silver nitrate and leaf extract solution (19:1, 17:3, 8:2 and 3:1) at 20 °C in a shaking incubator under dark conditions.

2.5. Characterizations

The reduction of pure Ag^+ ions was monitored by measuring UV–Vis spectrum of reaction solution at various time intervals as a function of temperature and concentration of extract. UV–visible spectral analysis has been achieved by using a Shimadzu UV-3101PC spectro photometer. The silver nanoparticles dispersed in water were placed on a carbon coated copper grid, excess was blotted after 5 min and grid was dried. Morphological images of the nanomaterials were analyzed using a transmission electron microscopy (HITACHI-JP/H7600) functioning at an accelerating voltage of 100 kV. The XRD grids were coated with dried biosynthesized nanoparticles and diffraction pattern of the synthesized nanoparticles was measured by a Rigaku X-ray powder diffractometer (XRD) with $Cu_{K\alpha}$ radiation ($\lambda = 0.1540$ nm). FTIR sample holder was placed with dried silver nanoparticles and KBr at a ratio of 5:95. FTIR spectrum of the synthesized silver nanoparticles was recorded at room temperature using a Perkin Elmer (model PE1600) spectrophotometer within the mid IR region of frequency 4000–400 cm^{-1} at a scan speed of 16 cm s^{-1}.

2.6. Bactericidal activity by disk diffusion method

The antibacterial activity of biosynthesized silver nanoparticles was tested by the disk diffusion method. Solid nutrient agar plates were spread with 100 µl suspensions of *S. typhimurium* (KCCM 11862) bacterial culture. Whatman filter paper

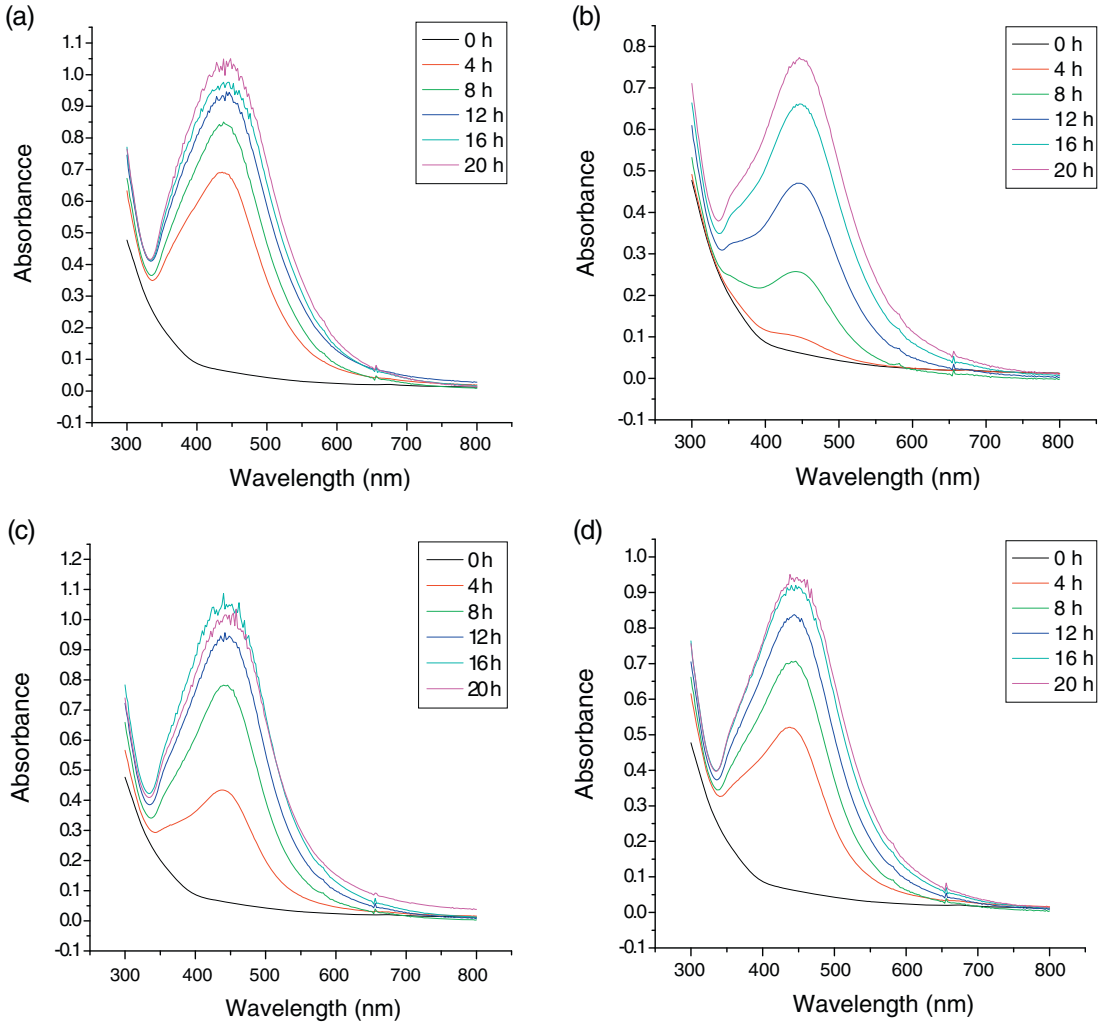

Figure 1 UV–Vis spectral analysis of silver nanoparticles at various time intervals synthesized at different temperatures (a) 20 °C, (b) 35 °C, (c) 50 °C and (d) 65 °C.

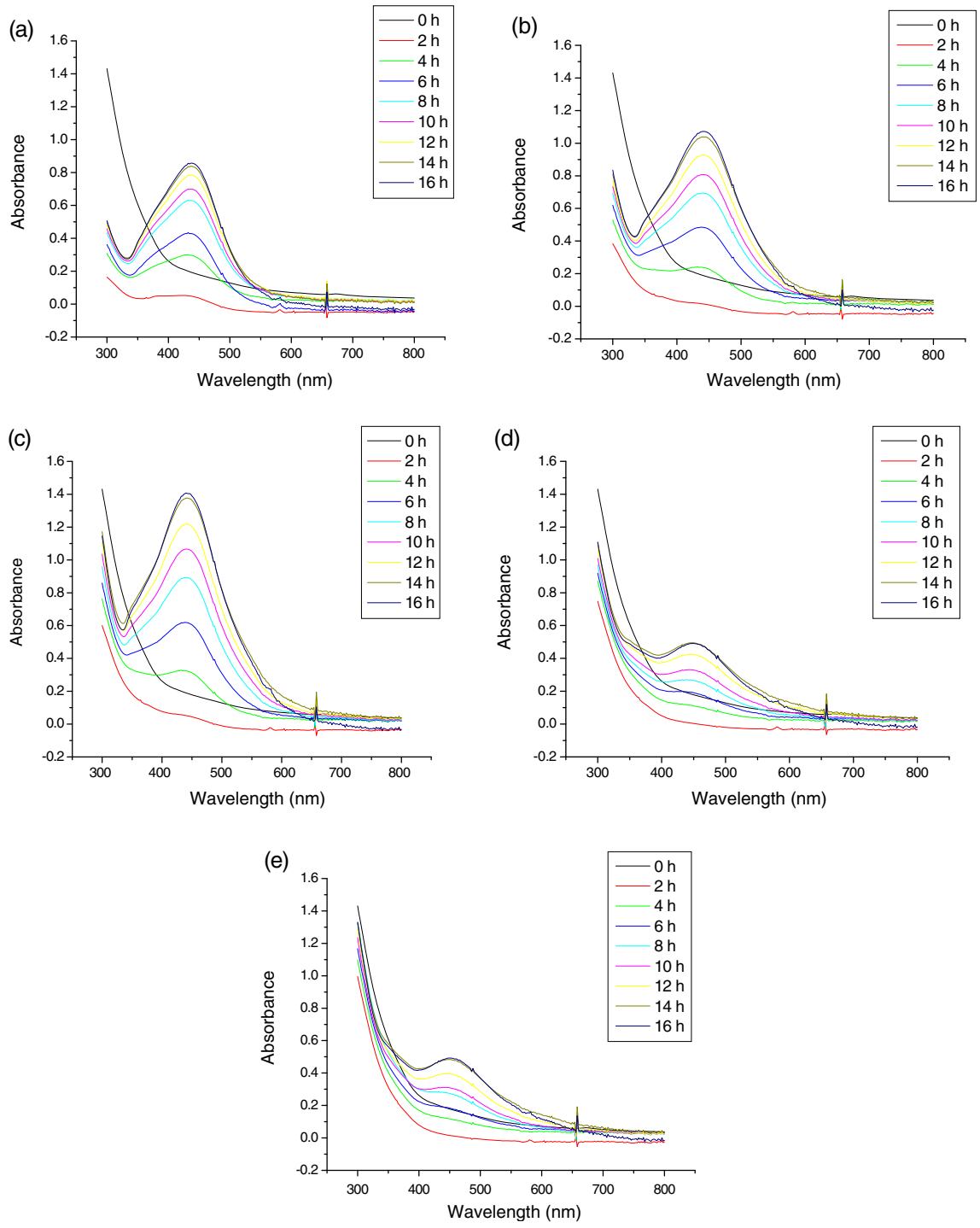

Figure 2 UV–Vis spectral analysis of silver nanoparticles synthesized at various time intervals using different concentrations of plant extract (a) 5%, (b) 10%, (c) 15%, (d) 20%, and (e) 25%.

(6 mm) disks were prepared and sterilized. The disks were loaded with 50, 100, 150 and 200 μg/disk concentrations of synthesized silver nanoparticles in solution and dried under sterile conditions. The dried disks were placed on inoculated plates and plates were incubated at 37 °C for 24 h. The diameters of inhibition zones were measured in millimeters. The tests were performed in triplicates.

2.7. Antibacterial activity in liquid cultures

The antibacterial activity of biosynthesized silver nanoparticles was studied using gram negative bacteria *S. typhimurium* cultured in a nutrient broth. The freshly cultured bacterium from nutrient agar plates was inoculated into the nutrient broth and incubated at 37 °C in a shaking incubator. The cultures obtained

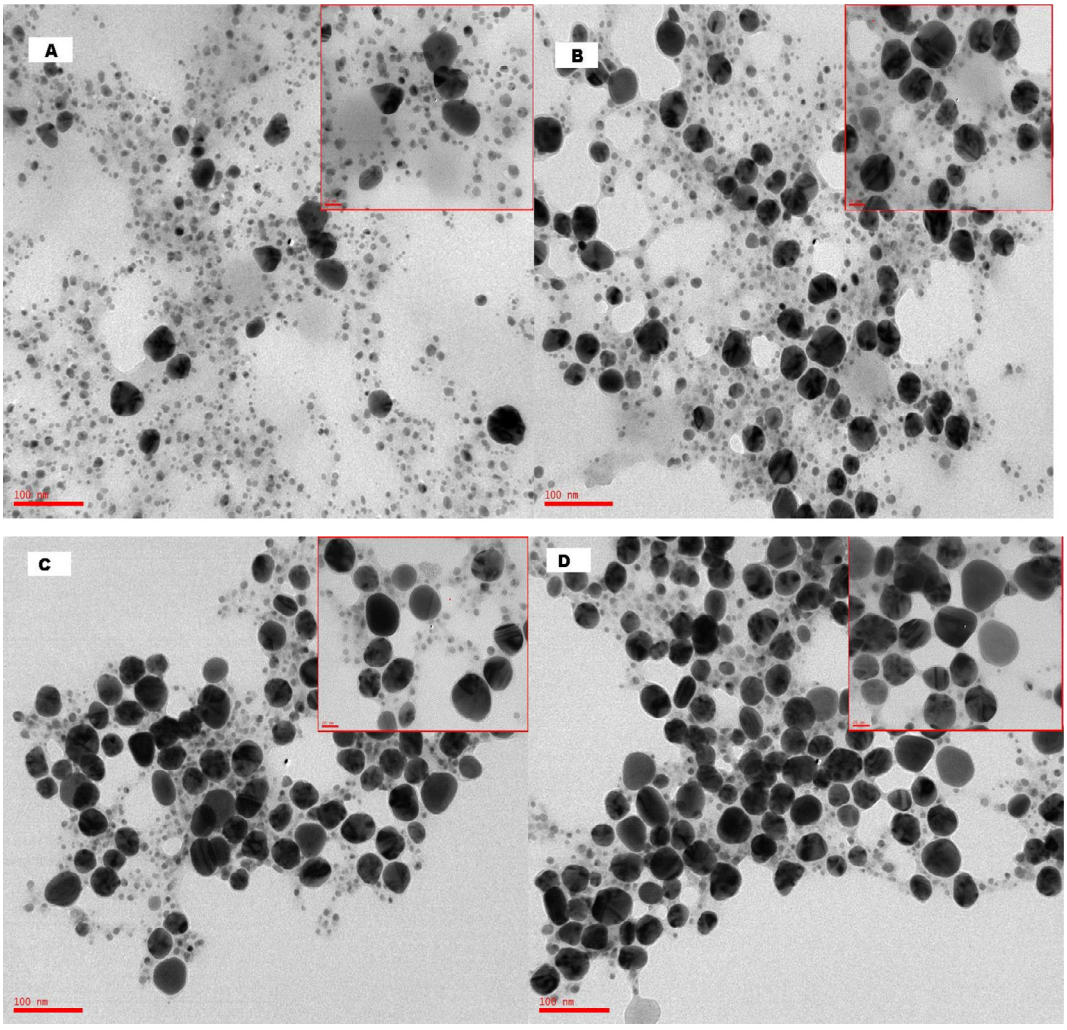

Figure 3 TEM images of silver nanoparticles synthesized at different temperatures (A) 20 °C, (B) 35 °C, (C) 50 °C and (D) 65 °C (outset images are at 100 nm scale and inset images at 20 nm scale).

after 12 h were used for further experiments. Thousand microliter of bacterial culture was inoculated into 50 ml of the nutrient broth containing the nanoparticles at different concentrations 150 and 200 μg/ml and incubated at 37 °C in a shaking incubator. The optical density was measured for every 4 h to determine the growth of the bacteria, using an UV–Vis spectrophotometer. The culture, without addition of nanoparticles was maintained as the control. The bacteria were collected by centrifugation, washed, coated on carbon grids and TEM analysis was performed.

3. Results and discussion

3.1. Silver nanoparticle biosynthesis

The biosynthesis of silver nanoparticles was performed using 45 ml of silver nitrate solution and 5 ml of extract. Change in color of solution from colorless to dark yellow or brown was observed for the formation of silver nanoparticles in the solution. The color change was noticed at 4th hour of incubation, indicating the beginning of formation of silver nano particles. The nanoparticles biosynthesized by the reduction of silver nitrate aqueous solution were analyzed by the UV–Vis spectroscopy to ensure formation and stability of silver nanoparticles in the solution. The peaks were found at 432, 438, 438 and 438 nm for silver nano particles synthesized at 20, 35, 50 and 65 °C, respectively. For 5, 10, 15, 20 and 25 ml of extract used to synthesize silver nanoparticles, the maximum absorption peaks were obtained at 424, 438, 436, 432 and 432 nm, respectively. The synthesis of silver nanoparticles occurred at 3rd–4th hour interval of addition of extract and completed within 24 h. As the time increased, the color intensity of solution increased with simultaneous increase in absorbance as represented in the Figs. 1 and 2.

The change in color from light yellow to brown was noticed at 4th hour of addition of plant extract to the silver nitrate solution. The peaks obtained within the 420–440 confirmed the biosynthesis of silver nanoparticles. The intensity of peaks increases with increase in the time, which indicated the generation of more and more nanoparticles and stability of the bio synthesized nanoparticles. The increase in absorbance was higher during time intervals 4–8 h and 8–12 h and later after 12 h increase in absorbance was observed but the rate was

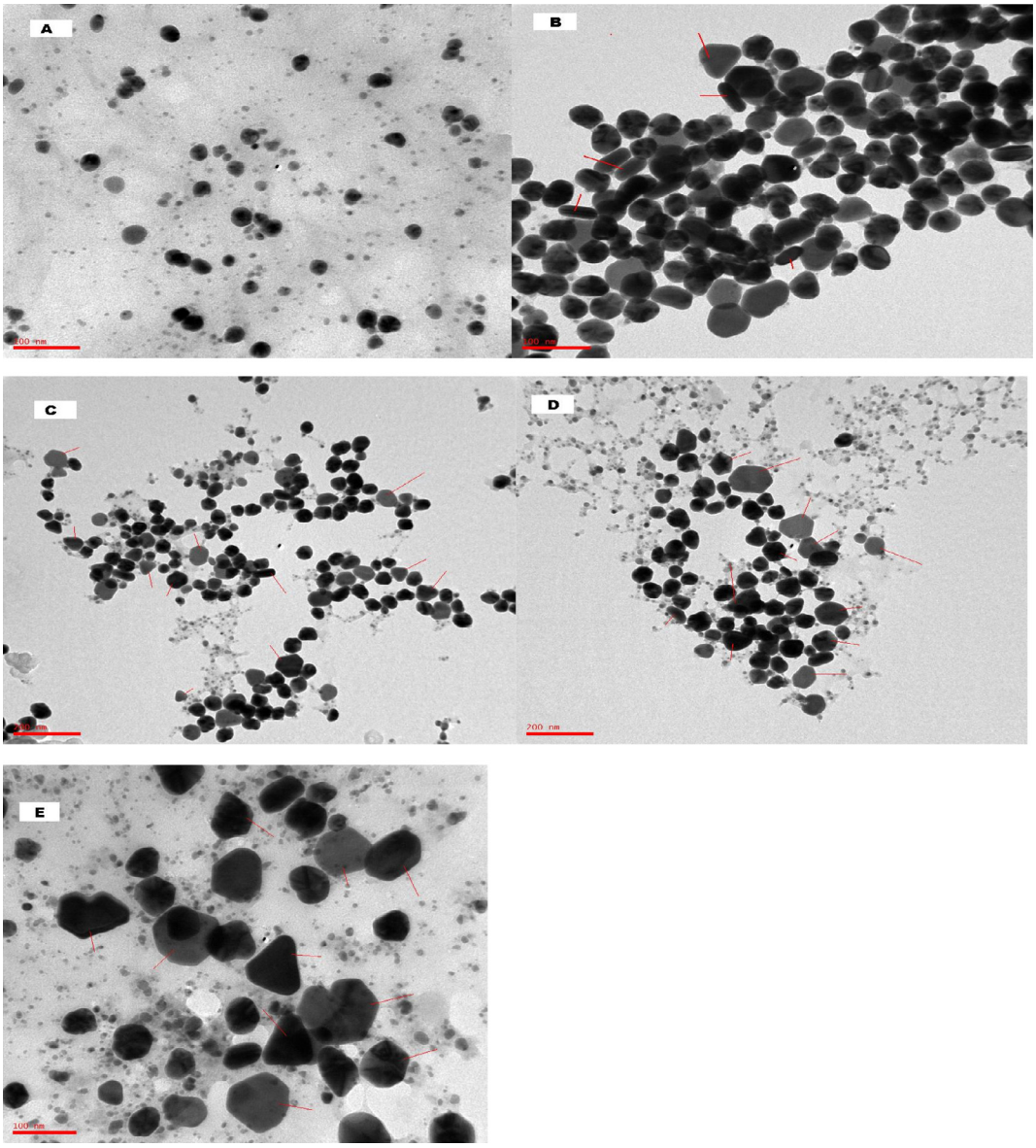

Figure 4 TEM images of nanoparticles obtained using various concentrations of the aqueous extract (A) 5 ml of extract, (B) 10 ml of extract, (C) 15 ml of extract, (D) 20 ml of extract and (E) 25 ml of extract. (Arrows indicate the non-spherical, plates).

slower as compared with the time interval 4–12 h. The increase in intensity could be attributed by reduction of silver nitrate to silver nanoparticles in the solution. This indicates that maximum production of nanoparticles at different temperatures was between 4 and 12 h. The maximum absorption peaks varied for samples incubated at various temperatures as well as for samples with varying concentrations of extract of *T. nucifera*. But the maximum absorption peak for nanoparticles synthesized at different temperatures did not vary much it was 432 nm for nanoparticles synthesized at 20 °C, 438 nm for nanoparticles biosynthesized at 35, 50 and 65 °C. As the temperature was increased, wavelength of maximum absorbance was also increased; which indicated the size dependence of nanoparticles with temperature. The intensity was observed to be higher for nanoparticles synthesized at lower temperature of 20 °C followed by 50, 65 and 35 °C.

Silver nanoparticles biosynthesized using various concentrations of aqueous extract revealed their effects on nanoparticle synthesis. Nanoparticles were successfully synthesized at all the five concentrations 5%, 10%, 15%, 20% and 25% of extract tested. But increased concentration of extract after particular concentration decreased the production of the nanoparticles, which could be noticed from intensity of the peaks obtained by UV–Visible spectroscopy as shown in Fig. 2. Increase in the concentration of extract from 5 to 10 and 15% increased the intensity of peaks indicating more production of silver nanoparticles, but further increase to 20% and 25% decreased the yield of synthesized nanoparticles and it was also relatively slow, which could be attributed by decreased concentration of silver nitrate in the solution. Increased production occurred with 10% and 15% extract is because of the availability of more amount of reducing agents

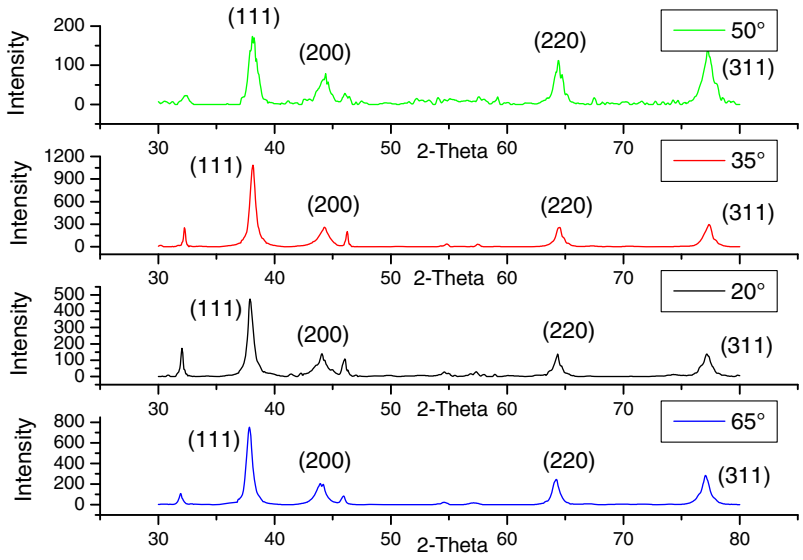

Figure 5 XRD pattern of silver nanoparticles synthesized at various temperatures 20 °C, 35 °C, 50 °C, and 60 °C using aqueous extract of *T. nucifera* with 1 mM $AgNO_3$.

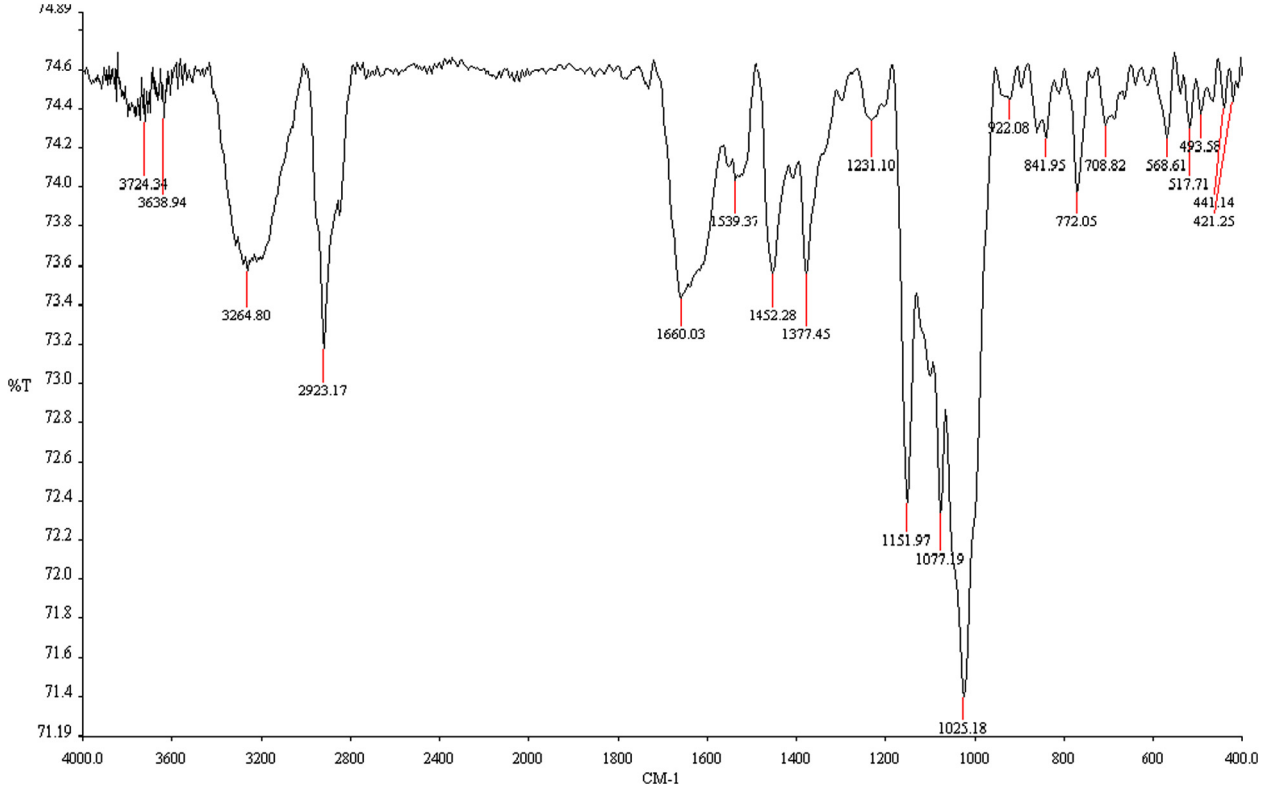

Figure 6 FTIR spectrum of silver nanoparticles synthesized using aqueous extract of *T. nucifera*.

from the aqueous extract of *T. nucifera*. The red shift of absorbance maximum was observed, when 10 ml of extract was used and blue shift occurred at the concentrations of 15, 20 and 25 ml but it was found to be lower for nanoparticles synthesized using 5 ml of the aqueous extract. According to He et al. (2008) as the size of nanoparticles increases their UV–Vis absorption peak would shift to red (He et al., 2008). But in our study much difference in the maximum absorbance was not observed with 10%, 15%, 20% and 25% of used extract for silver nanoparticle synthesis. As per the results obtained by Bio-TEM the minimum size of nanoparticles obtained was 10 nm with all concentrations of extract, which

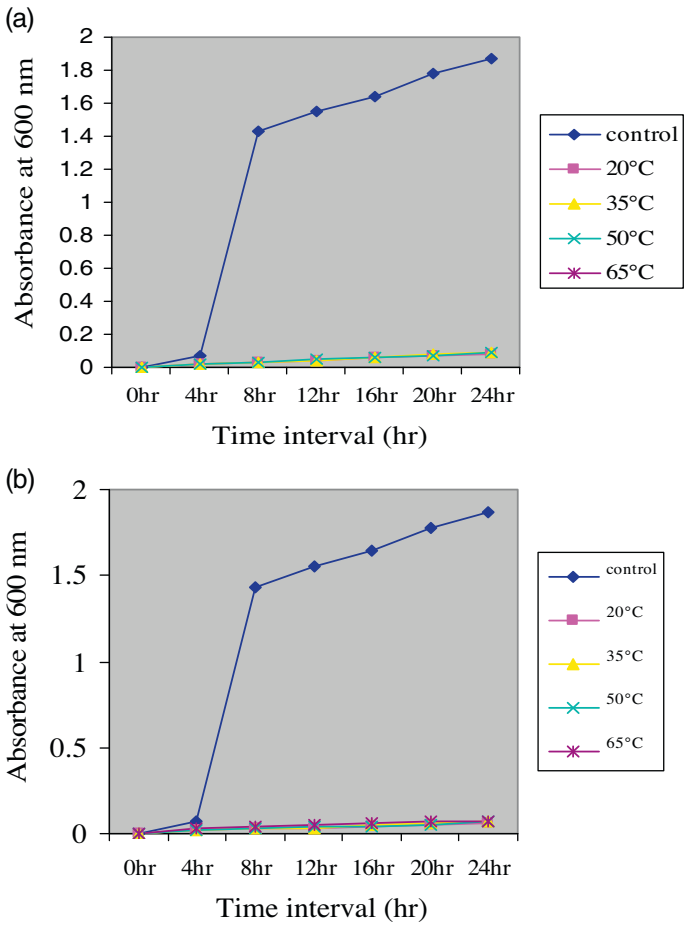

Figure 7 Growth curve of *S. typhimurium* in nutrient broth inoculated with bacteria at different concentrations of silver nanoparticles (a) 150 µg/ml and (b) 200 µg/ml.

could be the possible reason for smaller differences in the absorption maximum.

3.2. Influence of temperature and concentration of extract on the physical characteristics of the nanoparticles

Temperature was found to play an important role in determining the size of silver nanoparticles in the present study. The synthesis of silver nanoparticles at different temperatures 20, 35, 50 and 65 °C resulted in generation of nanoparticles of different sizes, whereas shape of the nanoparticles were not altered. The nanoparticles in size ranging between 5 and 15 nm were synthesized at 20 °C, whereas at temperatures 35, 50 and 65 °C, size of the nanoparticles were found to be between 10–45, 15–55 and 10–60 nm, respectively. The TEM images obtained for silver nanoparticles synthesized using aqueous extract of *T. nucifera* are shown in Fig. 3. The concentration of extract alters the shape and size of nanoparticles in the solution. The results obtained from TEM analysis of silver nanoparticles synthesized from various concentrations of extract, indicate variation in morphology. The size of the nanoparticles varied between 10–45, 10–75, 10–60, 10–80 and 10–125 nm for concentrations of 5, 10, 15, 20 and 25 ml extract used, respectively. The uniform spherical shaped particles were obtained for 5 ml extract used. As the concentration of extract was further increased, occurrence of rod shaped particles followed by formation of triangular and hexagonal shaped silver nanoparticles was noticed as depicted in Fig. 4.

Smaller sized nanoparticles were obtained at all operational temperatures, but the formation of larger sized nanoparticles was found to be proportional to temperature. Similar results were obtained with silver nanoparticles synthesized by synergetic reduction approach, where triangular shaped nanoplates increased in size from 90 to 180 nm with slight increase in temperature (Jiang et al., 2011). Increased concentration of extract in nanoparticle synthesis resulted in the formation of different shapes of nanoparticles. Additionally, for the spherical nano particles, it is purely attributed by the contribution of excess reducing agents present in aqueous extract. It leads to the aggregation of nanoparticles by interactions between capping molecules which encapsulated the nanoparticles and preformed nuclei (Song and Kim, 2009).

Studies by Jiang et al. suggested that the formation of different shapes of triangular nanoparticles is by fusion of two or more nuclei of different shapes, to form a cluster and gives either plate like or spherical particles (Jiang et al., 2011). The coexistence of nanoparticles of various shapes is also attributed by their necessity to form crystalline silver structure; face-centered-cubic (fcc) structure, which exhibits single, twin, or multiple plane structures leads to the coexistence of different morphologies.

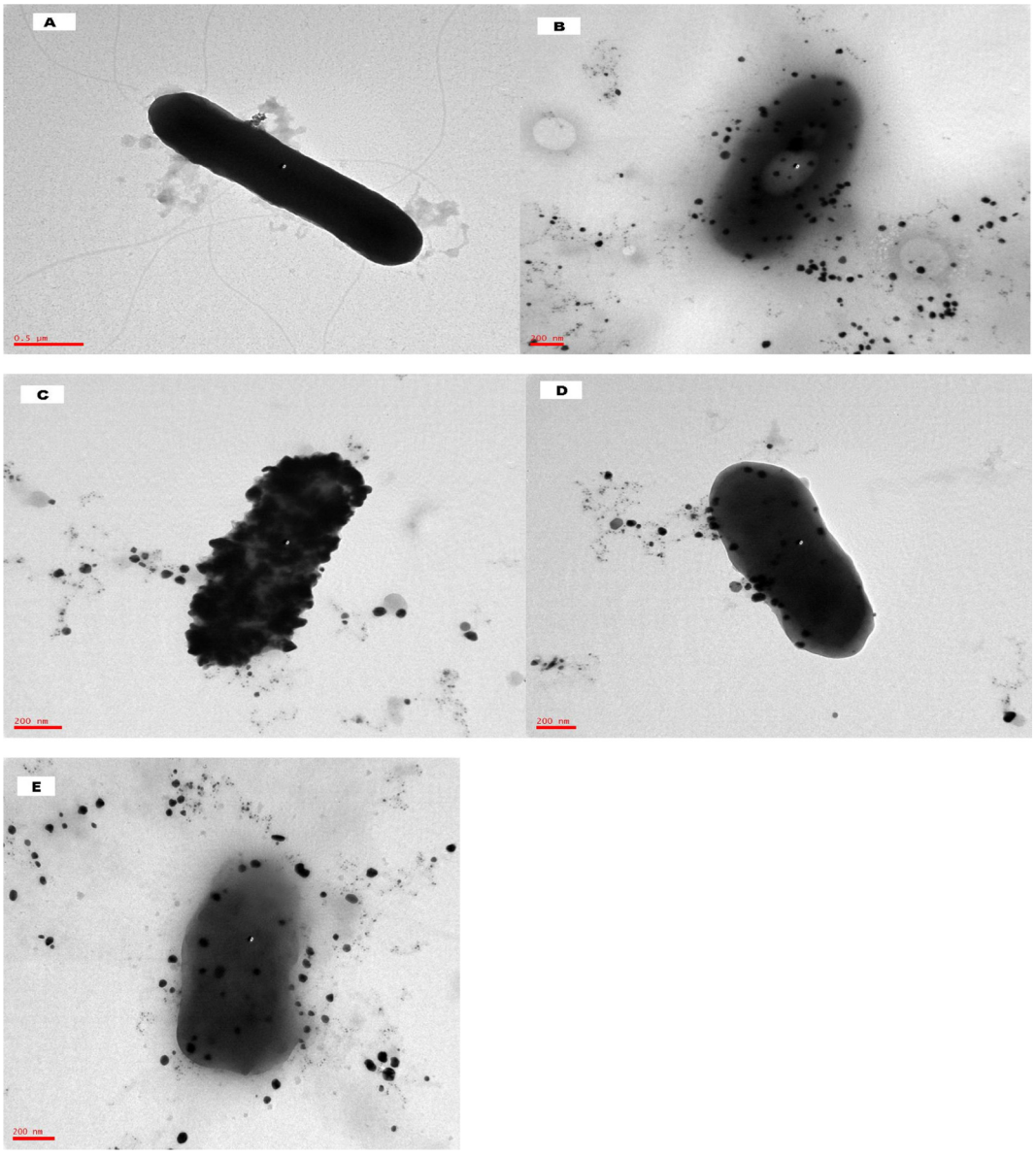

Figure 8 Action of silver nanoparticles on *S. typhimurium* as observed under TEM (A) normal *S. typhimurium* cell, (B and C) attachment of silver nanoparticles on the inner and outer membrane, (D) internalization of nanoparticles, (E) shrinkage of the cells leading to cell lysis.

3.3. XRD pattern of the synthesized silver nanoparticles

The X-ray diffraction patterns obtained for dried nanoparticles synthesized at different temperatures are shown in Fig. 5. To determine crystalline nature, size of nanoparticles and nature of the compounds involved in the stabilization of nanoparticles, XRD and FT-IR studies were carried out. The obtained XRD patterns confirmed the crystalline nature of synthesized silver nanoparticles. Four diffraction peaks were observed at 38.13, 44.3, 6.45 and 77.39° represent the (111), (200), (220) and (311), reflections and the face-centered cubic structure of metallic silver, respectively (JCPDS No. 04-0783). The crystallite sizes of silver nanoparticles were calculated for all obtained Bragg reflections (111), (200), (220) and (311) using JADE 9 software. The average grain size for silver nanoparticles synthesized at 20 °C was calculated to be 15.8, 17.9, 17.3 and 15.1 nm for the reflections (111), (200), (220) and (311), respectively. And for the particles formed at 35 °C, sizes were found to be 16.4, 11.7, 17.1, and 14.4 nm. The average grain sizes of 14.3, 14.0, 16.3, 13.8 nm and 15.8, 13.1, 16.7, 16.6 nm were found for nanoparticles synthesized at 50 and 65 °C, respectively. The crystallite size values obtained from XRD are found to be within the range of the particle size obtained by TEM analysis.

3.4. FT-IR analysis

The FTIR spectroscopy showed the bands at 3264, 2923, 1660, 1539, 1452, 1377, 1231, 1151, 1077 and 1025 cm^{-1} as shown in Fig. 6. The obtained FTIR spectrum for the biosynthesized nanoparticles, revealed that the proteins are the principle components involved in the encapsulation and stabilization

of synthesized silver nanoparticles. The peaks at 1660, 1539, 1231, 772 and 568 cm^{-1} can be assigned for amide I, II, III, V and VI N–H bending of peptide linkages of proteins, respectively (Kong and Yu, 2007). The O–H stretch band was represented by peak at 2923 cm^{-1}. The peaks at 708 and 1025 cm^{-1} may be due to the presence of C–S stretch (CH_2–S) of thiol or thioether and absorption peaks of –C–O–C bonds, respectively (Coates, 2000). Stabilization of silver nanoparticles using *Hibiscus rosa sinensis* was reported as the $–COO^-$ group of aminoacid residue in protein (Philip, 2010). The carbonyl groups of aminoacid residues and peptides of proteins can bind to metals strongly, and proteins were found to stabilize silver nanoparticles (Jain et al., 2011). The extract prepared at high temperatures such as 80 and 100 °C and extraction for long time were unsuccessful in synthesizing nanoparticles, which might be probably due to denaturation of proteins at higher temperatures and prolonged extraction. The FT-IR data suggest the proteins involved in capping and stabilization of the synthesized silver nanoparticles.

3.5. Antibacterial activity

The antibacterial activity of silver nanoparticles was tested against *S. typhimurium* by the agar diffusion method using 50, 100, 150 and 200 μg/disk of silver nanoparticles biosynthesized at various temperatures. Increased activity was observed with increase in concentrations, but significant difference in antibacterial activity between nanoparticles synthesized at various temperatures was not observed (data not shown). The antibacterial studies were performed in liquid cultures of *S. typhimurium* at concentrations of 150 and 200 μg/ml. Antibacterial activity for silver nanoparticles obtained at different temperatures is given in Fig. 7.

The antibacterial activity was performed with the nanoparticles synthesized at various temperatures to check the influence of size on antibacterial activity. But the results demonstrated that, silver nanoparticles synthesized at various temperatures did not show very much difference antibacterial activity against *S. typhimurium* because nanoparticles synthesized at various temperatures had an increase in size but at temperatures 20, 35, 50 °C nanoparticles of smaller sizes were predominant and relatively lower number of smaller sized nanoparticles at 65 °C. The smaller sized nanoparticles could gain easy entry into the bacterial cells. The gram positive bacteria have a thick peptidoglycan layer, whereas peptidoglycan layer in the gram negative bacteria is thin but surrounded by a lipid layer outside. The antibacterial activity of silver nanoparticles on *E. coli*, gram negative bacterium was suggested to be primarily by loss of permeability of outer membrane resulting in leakage of cellular materials, followed by entry into their inner membrane and finally damaging respiratory chain dehydrogenases, thereby preventing bacterial respiration and reproduction (Li et al., 2010). To determine the mechanism of antibacterial activity of silver nanoparticles synthesized using aqueous extract of *T. nucifera*, TEM analysis of bacteria treated with the synthesized silver nanoparticles was performed. *S. typhimurium* is a motile bacterium with peritrichous flagella, control cells show the presence of flagella, but bacterial cells treated with silver nanoparticles were found to lose their flagella. Fig. 8 depicts the attachment of nanoparticles on outer membrane of bacteria and entry of nanoparticles into their inner membrane. TEM photographs as depicted in Fig. 8 define the probable mechanism of action of silver nanoparticles synthesized using aqueous extract of *T. nucifera,* which is by attachment of nanoparticles onto membrane, followed by gaining entry into the cell, damaging membrane, further leading to leakage of cell constituents and shrinkage of cell.

4. Conclusions

The synthesis of silver nanoparticles by phytoreduction of silver nitrate yielded spherical, rod, triangular and irregular hexagonal shaped silver nanoparticles. Temperature was found to play a vital role in determining the size whereas concentration of extract was involved in determining the shape of nanoparticles. The increase in concentration of extract reduced the yield of silver nanoparticles. The biosynthesized nanoparticles were found to be stabilized by proteins; which contain no hazardous chemicals and are ecofriendly. The biosynthesized silver nano particles exhibited superior antibacterial activity against *S. typhimurium*, which validates its use as antibacterial agents in purification of water and can also be used as coating on food packaging to avoid contamination of *S. typhimurium*.

Acknowledgement

This research was supported by the National Research Foundation of Korea (NRF) grant 1101000369 funded by the Korea government.

References

Ailes, E., Budge, P., Shankar, M., Collier, S., Brinton, W., Cronquist, A., Chen, M., Thornton, A., Beach, M.J., Brunkard, J.M., 2013. PLoS ONE 8 (3), e57439.
Ali, D.M., Sasikala, M., Gunasekaran, M., Thajuddin, N., 2011. Dig. J. Nanomater. Biostruct. 6, 385–390.
Ahmad, A., Mukherjee, P., Senapathi, S., Mandal, D., Khan, M.I., Kumar, R., Sastry, M., 2003. Colloids Surf., B 28, 313–318.
Amato, E., Diaz-Fernandez, Y.A., Taglietti, A., Pallavicini, P., Pasotti, L., Cucca, L., Milanese, C., Grisoli, P., Dacarro, C., Fernandez-Hechavarria, J.M., Necchi, V., 2011. Langmuir 27, 9165–9173.
Avasthi, D.K., Mishra, Y.K., Kabiraj, D., Lalla, N.P., Pivin, J.C., 2007. Nanotechnology 28 (12), 125604.
Bae, K.H., 2000. The Medicinal Plants of Korea. Kyo-Hak Publishing Co. Ltd., 45.
Capek, I., 2004. Adv. Colloid Interface Sci. 110, 49–74.
Cao, X.L., Cheng, C., Ma, Y.L., Zhao, C.S., 2010. J. Mater. Sci. Mater. Med. 21, 2961–2964.
Chernousova, S., Epple, M., 2013. Angew. Chem. Int. Ed. 52, 1636–1653.
Chandran, S.P., Chaudhary, M., Pasricha, R., Ahmad, A., Sastry, M., 2006. Biotechnol. Prog. 22, 577–583.
Coates, J., 2000. Interpretation of Infrared Spectra, A Practical Approach Encyclopedia of Analytical Chemistry. John Wiley & Sons Ltd., Chichester, 15.
Dwivedi, A.D., Gopal, K., 2010. Colloids Surf. Physicochem. Eng. Aspects 369, 27–33.
Dubey, S.P., Lahtinen, M., Sillanppa, M., 2010. Colloids Surf., A 364, 34–41.
Gajbhije, M., Kesharwani, J., Ingle, A., Gade, A., Rai, M., 2009. Nanomed. Nanotechnol. Biol. Med. 5, 382–386.
Hetrick, E.M., Schoenfisch, M.H., 2006. Chem. Soc. Rev. 35, 780–789.
Huang, J., Li, Q., Sun, D., Lu, Y., Su, Y., Yang, X., Wang, H., Want, Y., Shao, W., He, N., Hong, J., Cuixue, C., 2007. Nanotechnology 18, 104–108.

He, S.T., Liu, Y.L., Maeda, H., 2008. J. Nanopart. Res. 10, 209–215.
Hu, Z., Zhang, J., Chan, W.L., Szeto, Y.S., 2006. J. Appl. Polym. Sci. 108, 52–56.
Jong, W.H.D., Born, P.J.A., 2008. Int. J. Nanomed. 3, 133–149.
Jain, P., Pradeep, T., 2005. Biotechnol. Bioeng. 90, 59–63.
Jain, N., Bhargava, A., Majumdar, S., Tarafdar, J.C., Panwar, J., 2011. Nanoscale 3, 635–641.
Jang, Y.P., Kim, S.R., Kim, Y.C., 2001. Planta Med. 67, 470–472.
Jiang, X.C., Chen, W.M., Chen, C.Y., Xiong, S.X., Yu, A.B., 2011. Nanoscale Res. Lett. 6 (32), 1–9.
Kowshik, M., Ashtaputre, S., Kharrazi, S., Urban, J., Kulkarni, S.K., Paknikar, K.M., 2003. Nanotechnology 1, 95–100.
Kong, J., Yu, S., 2007. Acta Biochim. Biophys. Sin. 39, 549–559.
Kim, S., Kim, H.J., 2006. Int. Biodeterior. Biodegrad. 57, 155–162.
Lee, W.S., Kim, J.R., Han, J.M., Jang, K.C., Sok, D.E., Jeong, T.S., 2006. J. Agric. Food Chem. 54, 5369–5374.
Li, W.R., Xie, B.X., Shi, Q.S., Zeng, H.Y., Ou-Yang, Y.S., Chen, Y.B., 2010. Appl. Microbiol. Biotechnol. 85, 1115–1122.
Mazur, M., 2004. Electrochem. Commun. 6, 400–403.
Mishra, Y.K., Mohapatra, S., Chakravadhanula, V.S.K., Lalla, N.P., Zaporojtchenko, V., Avasthi, D.K., Faupel, F., 2010. Nanosci. Nanotechnol. 10 (4), 2833–2837, 5.
Mishra, Y.K., Mohapatra, S., Kabiraj, D., Lalla, N.P., Pivin, J.C., Avasthi, D.K., 2007. Scr. Mater. 56 (7), 629–632.
Morones, J.R., Elechiguerra, J.L., Camacho, K., Holt, J., Kouri, J.B., Ramirez, J.Y., Yacaman, M.J., 2005. Nanotechnology 16, 2346–2353.
Pallavicini, P., Dacarro, G., Diaz-Fernandez, Y.A., Taglietti, A., 2014. Coord. Chem. Rev. 275, 37–53.
Pal, S., Tak, Y.K., Song, J.M., 2007. Appl. Environ. Microbiol. 73, 1712–1720.
Philip, D., 2010. Physica E 42, 1417–1424.
Parashar, V., Parashar, R., Sharma, B., Pandey, A.C., 2009. Dig. J. Nanomater. Biostruct. 4, 45–50.
Ratyakshi, Chauhan, R.P., 2009. Asian J. Chem. 21, 113–116.
Reddy, A.S., Chen, C.M., Chen, C.C., Jeans, J.S., Chen, H.R., Tseng, M.J., Fan, C.W., Wang, J.C., 2010. J. Nanosci. Nanotechnol. 10, 6567–6574.
Ryu, Y.B., Jeong, H.J., Kim, J.H., Kim, Y.M., Parl, J.Y., Kim, D., Naguyen, T.T.H., Park, S.J., Chang, J.S., Park, K.H., Rho, M.C., Lee, W.S., 2010. Bioorg. Med. Chem. 18, 7940–7947.
Saifuddin, N., Wong, C.W., Nur Yasumira, A.A., 2009. Eur. J. Chem. 6, 61–70.
Saint, S., Elmore, J.G., Sullivan, S.D., Emerson, S.S., Koepsell, T.D., 1998. Am. J. Med. 105, 236–241.
Shankar, S.S., Rai, A., Ahmad, A., Sastry, M., 2004. J. Colloid Interface Sci. 275, 496–502.
Sharma, V.K., Yngard, R.A., Lin, Y., 2009. Adv. Colloid Interface Sci. 145, 83–96.
Sileikaite, A., Prosycev, I., Puiso, J., Juraitis, A., Guobiene, A., 2006. Mater. Sci. 12, 287–291.
Singhal, R., Agarwal, D.C., Mishra, Y.K., Singh, F., Pivin, J.C., Chandra, R., Avasthi, D.K., 2009. J. Phys. D Appl. Phys. 42 (15), 155103.
Song, J.Y., Kim, B.S., 2009. Bioprocess Biosyst. Eng. 31, 79–84.
Solomon, S.D., Bahadory, M., Jeyarajasingam, A.V., Rutkowsky, S.A., Charles, B., 2007. J. Chem. Educ. 84, 322–325.
Wiley, B., Sun, Y., Xia, Y., 2007. Acc. Chem. Res. 40, 1067–1076.
Zielinska, A., Skwarek, E., Zaleska, A., Gazda, M., Hupka, J., 2009. Procedia Chem. 1 (15), 60–1566.